Desalination and Water Treatment
www.deswater.com

doi: 10.5004/dwt.2022.27961

245 (2022) 144–157
January

Optimization of activated carbon by chemical activation from grape seeds using the response surface methodology

Safae El Alami El Hassani, Anas Driouich*, Hassan Chaair, Hamid Mellouk, Khalid Digua

Laboratory of Process Engineering and Environment, Faculty of Sciences and Technology, University Hassan II, Mohammedia, BP 577, Morocco, emails: anasdriouich23@gmail.com (A. Driouich), alamihassanisafae@gmail.com (S.E.A. El Hassani), hchaair@yahoo.fr (H. Chaair), hmellouk@gmail.com (H. Mellouk), k.digua@gmail.com (K. Digua)

Received 9 June 2021; Accepted 29 October 2021

ABSTRACT

Activated carbon from grape seed was prepared using the chemical activation method, which consisted of treatment by potassium hydroxide (KOH). Factors influencing the activated carbon preparation were particle size, impregnation ratio, final temperature, heating rate, and the activating agent concentration were studied by using a central composite design. The methodology chosen in this paper is based on the use of a polynomial model to express the responses, yield of activated carbon synthesized, and adsorbed amount of methylene blue as a function of the five influencing factors. The significance of the factors was studied by analysis of variance using the Fisher test, linear effects diagram, response surface curves, and iso-response curves. According to the Response Surface Methodology, optimal conditions for the preparation of activated carbon have been identified to be a particle size of 300 μm, an impregnation ratio of 0.15, a final temperature of 650°C, a heating rate of 10°C/min and an activating agent concentration of 35%. Under these conditions, the synthesis yield of AC and 40%, while the adsorption capacity of methylene blue was 492 mg/g. The characteristics of activated carbon obtained under these experimental conditions were by FTIR analysis indicate the presence of a variety of functional groups on the surface of activated carbon. These results demonstrated that the grape seeds are a suitable precursor for the production of activated carbon.

Keywords: Grape seeds; Activated carbon; Chemical activation; Adsorption; Optimization; Response surface methodology

1. Introduction

The increase in agricultural and industrial activities generates huge quantities of waste of different kinds and whose management is still a concern for specialists [1]. Grape is one of the most and the oldest fruits it was exclusively cultivated for producing wine. Grape waste generated by the processing units consists of pulp, stalks and pips. These are used for the extraction of oil which has become highly exploited because of its chemical composition [2]. Grape seeds oil owes its antioxidant qualities to its high content of vitamin E and polyphenols, and linoleic acid (fatty acid from the omega-6 family) which are good for protecting the epidermis from dehydration [3–5]. Grape seeds pomace abandoned is a source of pollution, therefore the recovery of this waste is a real opportunity for the development of environmental protection. They found applications in the production of activated carbon for residues such as palm shell, wood biomass, waste palm, and coconut and peanut shell [6–10]. Activated carbon are adsorbents widely used for the elimination of pollutants [11].

* Corresponding author.

They are composed of carbon atoms organized within graphite structure, characterized by a large sorption capacity and a porous structure, and a large specific surface that can reach 3100 m^2/g [12]. Activated carbon is used to eliminate pollutants and odors from liquid and gaseous phases and in the medical field [13,14]. They are used as catalysis [15] and for gas storage [16]. Electrode materials in electrochemical devices [17]. Elimination of organic pollutants from drinking water and wastewater treatment [18].

However, commercial activated carbon costs were very high it became necessary to find an alternative solution. Recently, some agricultural waste, such as pumpkin rind and palm shell were used to prepare activated carbon [19,20]. In the literature, they are two methods that are used to produce activated carbon, physical activation and chemical activation [6,12,13]. Based on previous works, chemical activation was chosen to prepare the activated carbon in this paper. It was chosen for its advantages it is simple with a shorter production time, lower activation temperature, and good development of porous structure and it is characterized by high yield [21,22].

Several parameters can affect the synthesis of activated carbon from grape seed, such as particle size, activation temperature, the activating agent concentration which is indicate the rate the activating agent, and impregnation ratio which is depends on the mass of grape seeds and the activating solution. The efficiency of the process can be increased by optimizing these factors [23]. Usually, to study the effect of factors on the production of activated carbons, several factors must be fixed at a certain level. While varying each other to determine the best condition for this parameter. However, the disadvantage of this method is that there is a lack of determination of the interactions between the studied factors which are essential to determine the characteristics of activated carbons [22,23]. To solve this problem, we chose to use an experimental design based on the response surface methodology (RSM) [24–26].

In this study, the response surface methodology (RSM) based on the design of a central composite design (CCD) was used to evaluate and optimize the effect of particle size, impregnation ratio, carbonization temperature, heating rate, and concentration of the activating agent as independent variables on the yield and adsorption capacity measured by the methylene blue of the activated carbon produced [24].

2. Materials and methods

2.1. Experimental procedures

Grape seed cake obtained after oil extraction was used as raw material to produce activated carbon by chemical activation using potassium hydroxide (KOH) as an activated agent followed by carbonization. Seeds were obtained from a Western region in Morocco. Oil was extracted using a pressed oil, the resulting cake was crushed and degreased with Soxhlet by using hexane as a solvent for 2 h. Then, the material was washed dried, and sieved. The fixed carbon yield was calculated at 91%.

Various vibrational frequencies, in the range of 4,000–400 cm^{-1} of grape seeds, are presented in Fig. 1. The IR spectrum of dried grape seeds show a strong and broad band at 3,421 cm^{-1} due to the presence of the OH stretching frequency of the hydrogen donor substituents (hydroxyl groups), attached to the aromatic ring structures of the flavonoid compounds in the grape seeds. The amide II band appears as a very strong band at 1,627 cm^{-1} [30]. The medium width band at 1,315–1,441 cm^{-1} is the N–H stretching mode [29]. The C–O–C and C–OH vibrations of the protein in the grape seeds appear as a very strong IR band at (1,072 cm^{-1}) [30].

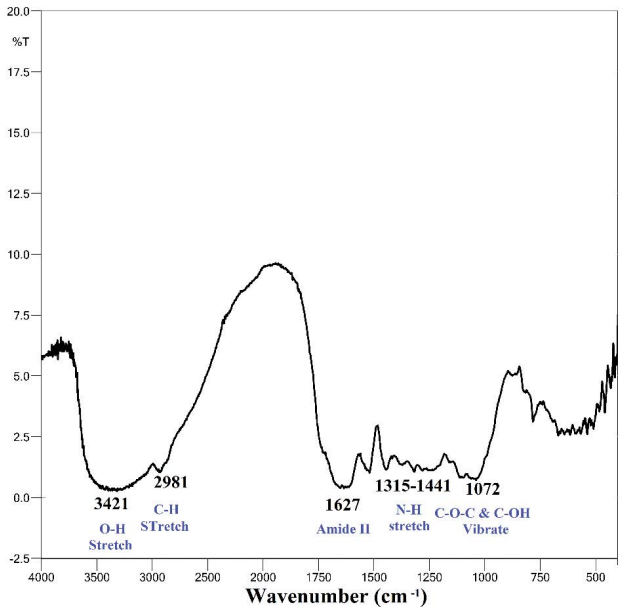

Fig. 1. Infrared absorption spectrum of grape seeds.

Initially, 8 g of dried raw material was impregnated in potassium hydroxide solutions with different concentrations, at different impregnation ratios under stirring at 60°C for 2 h. The impregnated samples were dried at 105°C for 24 h. The dried material was placed in a ceramic crucible which was inserted into a muffle furnace, to be carbonized at an inert atmosphere heated at a rate between 5°C/min and 20°C/min, and held at a different temperature varying between 500°C to 900°C.

After carbonization, activated carbon produced was washed with concentrate solution of hydrochloric acid before being washed with distilled water until the residual water reached a pH between 6 and 7. Finally, the AC samples were dried at 105°C for 24 h then they were sieved and stored in glass flasks (Fig. 1) [21].

2.2. Analytical methods

2.2.1. Activated carbon yield (%)

Activated carbon yield allows us to estimate the quantities of AC that can be obtained from an initial quantity of dry biomass. Then, the yield was calculated from the ratio of AC mass to the mass of the impregnated biomass.

$$\text{Activated carbon yield}(\%) = \frac{\text{final mass}}{\text{initial mass}} \times 100 \quad (1)$$

2.2.2. Methylene blue adsorption capacity (mg/g)

The adsorption capacity of AC obtained was determined by measuring the adsorption capacity of methylene blue. Then, 0.1 g of AC samples were added to 100 mL of MB solution at 0.05 g/L and the mixture was stirred for 1 h at room temperature. Then, the mixture was filtered.

After adsorption, to determine the amount of methylene blue adsorbed it is necessary to determine the residual concentration of methylene blue solution using the UV-visible spectrophotometer at λ = 664 nm. A calibration curve was given, and the adsorption capacity was calculated as the following formula [27].

$$\mathrm{QMB} = \frac{\left[C_0 - C\right]}{\mathrm{mac}} \times V \tag{2}$$

where C_0 : Initial concentration (50 mg/L), C: Residual concentration (mg/L), mac: Mass of activated carbon (g), V: Volume of MB (100 mL).

2.3. Central composite design

The synthesis of activated carbon prepared from grape seeds was optimized using the design of experiments methodology. A central composite design was chosen to relate two studied responses, activated carbon yield (%) and methylene blue adsorption capacity (mg/g), affected by five factors, particle size, impregnation ratio, final temperature, heating rate, and activating agent concentration.

Optimal values for the operating parameters were estimated by analyzing the response surface curves and isoresponse curves of the dependent variables (Y_1: Activated carbon yield (%) and Y_2: Methylene blue adsorption (mg/g)) as a function of the independent variables. The range and levels of the independent variables are listed in Table 1.

To obtain a good descriptive quality of the model and to allow a reliable prediction in the whole experimental field considered, and for a reasonable number of manipulations, the realization of the central composite design requires a number of tests equal to 36:

$$2^k + 2k + N_0 = 16 + 10 + 10 = 36 \tag{3}$$

where K is the number of variables and N_0 is the number of repetitions of the central point. Table 2 brings together the set of 36 tests, defining the matrix of experiments for the different factors considered. The ith line of this matrix defines the experimental conditions of the ith experiment [28].

All the operating conditions are performed in a randomized order, and the results obtained after experimentation are grouped in Table 2.

The concept of the exploitation of the results is based on the analysis of variance of the regression, the estimation of coefficients of the models, their significance concerning the experimental error, and the calculation of the residuals [26]. Statistical analysis was performed by using JMP [29] and STATISTICA [30] software.

3. Results and discussion

3.1. Variance analysis

The analysis of variance shows whether the variables selected for modeling have a significant effect as a whole on the response [31,33]. The results of the analysis of variance are summarized in Table 3.

It can be seen that both models explain perfectly the experimental results. In fact, the value of the experimental value of Fisher for the response 'Activated carbon yield (%) (F_{exp} = 9.2097) and the Methylene blue adsorption response (F_{exp} = 15.9862)' are higher than the critical value of Fisher factor ($F_{0.01}(20,15)$ = 5.25) [32] at a 99.9% confidence level. Consequently, the factors used for modeling are significant overall.

3.2. Statistical study of factors effects

Recall that a factor is significant at 5%, 1%, or 0.1% when its experimental estimated Fisher value (F_{exp}) is higher than or equal to the critical Fisher value (F_c) at a 95%, 99%, or 99.9% confidence level [30,32].

Tables 4 and 5 show the values of model coefficients, their significances, and their effects. Analysis of the results in these tables shows that:

For the first response (AC yield) and a 99% confidence level, the particle size P_s, the impregnation ratio I_R and the final temperature F_T showed significant linear effects.

Table 1
Independent variables, experimental range and levels

Natural variables (X_i)	Symbol	Coded variables X_1, X_2, X_3, X_4, X_5					Δx
		$-\alpha$	–1	0	1	$+\alpha$	
X_1 = Particle size (μm)	P_s	125	200	275	350	425	75
X_2 = Impregnation ratio (g/mL)	I_R	0.045	0.14	0.235	0.33	0.425	0.095
X_3 = Final temperature (°C)	F_T	500	600	700	800	900	100
X_4 = Heating rate (°C/min)	H_r	4	8	12	16	20	4
X_5 = AA concentration (%)	[AA]	10	20	30	40	50	10

α = 2.00, $X_i = \dfrac{x_i - x_0}{\Delta x_i}$

Table 2
Central composite design and experimental results for activated carbon yield (%) and Methylene blue adsorption capacity (mg/g)

Rand order	Actual order	Factors					Responses*	
		G	R_I	T	P_v	[AA]	Y_1 (%)	Y_2 (mg/g)
18	1	–1	–1	–1	–1	–1	14.98	470.61
14	2	–1	–1	–1	1	1	14.72	497.47
22	3	–1	–1	1	–1	1	19.92	497.79
25	4	–1	–1	1	1	–1	20.22	495.97
32	5	–1	1	–1	–1	1	26.31	434.67
28	6	–1	1	–1	1	–1	21.75	442.26
33	7	–1	1	1	–1	–1	11.65	499.37
24	8	–1	1	1	1	1	3.6	496.45
29	9	1	–1	–1	–1	1	25.91	484.28
19	10	1	–1	–1	1	–1	49.71	484.52
9	11	1	–1	1	–1	–1	19.42	493.36
12	12	1	–1	1	1	1	41.67	482.6
34	13	1	1	–1	–1	–1	28.26	448.1
13	14	1	1	–1	1	1	21.89	487.99
8	15	1	1	1	–1	1	11.75	494.94
7	16	1	1	1	1	–1	13.04	496.05
30	17	–2	0	0	0	0	29.34	487.89
11	18	2	0	0	0	0	35.44	476.93
26	19	0	–2	0	0	0	31.32	487.99
6	20	0	2	0	0	0	26.26	474.56
31	21	0	0	–2	0	0	30.28	467.68
4	22	0	0	2	0	0	3.37	497.31
20	23	0	0	0	–2	0	15.51	486.13
16	24	0	0	0	2	0	9.8	494.94
1	25	0	0	0	0	–2	22.09	484.73
3	26	0	0	0	0	2	27.6	496.52
10	27	0	0	0	0	0	28.7	498.1
17	28	0	0	0	0	0	29.75	493.14
21	29	0	0	0	0	0	31.36	496.6
23	30	0	0	0	0	0	31.44	496.05
27	31	0	0	0	0	0	29.6	493.36
15	32	0	0	0	0	0	31.67	494.15
5	33	0	0	0	0	0	26.96	495.18
2	34	0	0	0	0	0	28.02	495.89
32	35	0	0	0	0	0	30.82	496.68
32	36	0	0	0	0	0	29.06	495.97

*Y_1: Activated carbon yield (%); Y_2: Methylene blue adsorption capacity (mg/g).

Table 3
Variance analysis of activated carbon yield and Methylene blue adsorption capacity models

	Source	Degree of freedom	Sum of squares	Mean square	$F_{\text{Statistics}}$	Prob. > F
AC yield (%)	Model	20	3,135.7699	156.788	9.2097	<0.0001*
	Residual	15	255.3654	17.024		
	Total	35	3,391.1353			
MB adsorption (mg/g)	Model	20	8,526.8254	426.341	15.9862	<0.0001*
	Residual	15	400.0400	26.669		
	Total	35	8,926.8654			

$F_{\text{statistics}}$: Experimental Fisher factor;
*: Significant to 0.1% ($F_{0.001}(20,15) = 5.25$).

Table 4
Result of multiple linear regression and coefficient estimation of activated carbon yield

Model term	Estimation	Sum of squares	$F_{Statistics}$	Prob. > F	Significance
Constant	29.725972	–	–	<0.0001	***
P_s	3.7791667	342.77042	20.1341	0.0004	***
I_R	–3.2675	256.23735	15.0512	0.0015	**
F_T	–4.836667	561.44027	32.9786	<.0001	***
H_r	0.7075	12.01335	0.7057	0.4141	NS
[AA]	–0.093333	0.20907	0.0123	0.9132	NS
$P_s - I_R$	–3.4525	190.71610	11.2025	0.0044	**
$P_s - F_T$	–1.095	19.18440	1.1269	0.3052	NS
$I_R - F_T$	–3.38	182.79040	10.7370	0.0051	**
$P_s - H_r$	3.34625	179.15823	10.5236	0.0054	**
$I_R - H_r$	–3.98625	254.24303	14.9341	0.0015	**
$F_T - H_r$	0.19875	0.63202	0.0371	0.8498	NS
P_s – [AA]	–0.3225	1.66410	0.0977	0.7589	NS
I_R – [AA]	–0.565	5.10760	0.3000	0.5919	NS
F_T – [AA]	2.405	92.54440	5.4360	0.0341	*
H_r – [AA]	–2.02625	65.69102	3.8586	0.0683	NS
$P_s - P_s$	0.6810417	14.84217	0.8718	0.3652	NS
$I_R - I_R$	–0.218958	1.53417	0.0901	0.7681	NS
$F_T - F_T$	–3.210208	329.77400	19.3707	0.0005	***
$H_r - H_r$	–4.252708	578.73690	33.9946	<.0001	***
[AA] – [AA]	–1.205208	46.48087	2.7303	0.1192	NS

***: Significant to 0.1% ($F_{0.001}(1,15) = 16.59$); **: Significant to 1% ($F_{0.01}(1,15) = 8.68$);
*: Significant to 5% ($F_{0.05}(1,15) = 4.54$); NS: Not significant.

Table 5
Result of multiple linear regression and coefficient estimation of methylene blue adsorption capacity

Model term	Estimation	Sum of squares	$F_{Statistics}$	Prob. > F	Significance
Constant	495.65701	–	–	<0.0001	***
P_s	0.63875	9.7920	0.3672	0.5536	NS
I_R	–5.567917	744.0407	27.8987	<0.0001	***
F_T	11.07875	2,945.7288	110.4538	<.0001	***
H_r	3.2420833	252.2665	9.4590	0.0077	*
[AA]	2.8970833	201.4342	7.5530	0.0149	*
$P_s - I_R$	4.463125	318.7118	11.9505	0.0035	**
$P_s - F_T$	–5.156875	425.4938	15.9544	0.0012	**
$I_R - F_T$	8.809375	1,241.6814	46.5584	<.0001	***
$P_s - H_r$	0.048125	0.0371	0.0014	0.9708	NS
$I_R - H_r$	1.946875	60.6452	2.2740	0.1523	NS
$F_T - H_r$	–5.560625	494.7288	18.5505	0.0006	***
P_s – [AA]	0.600625	5.7720	0.2164	0.6485	NS
I_R – [AA]	0.661875	7.0093	0.2628	0.6157	NS
F_T – [AA]	–4.493125	323.0108	12.1117	0.0034	**
H_r – [AA]	2.841875	129.2201	4.8453	0.0438	*
$P_s - P_s$	–3.493021	390.4382	14.6400	0.0017	**
$I_R - I_R$	–3.776771	456.4479	17.1151	0.0009	***
$F_T - F_T$	–3.471771	385.7022	14.4624	0.0017	**
$H_r - H_r$	–1.461771	68.3768	2.5639	0.1302	NS
[AA] – [AA]	–1.439271	66.2880	2.4856	0.1357	NS

***: Significant to 0.1% ($F_{0.001}(1,15) = 16.59$); **: Significant to 1% ($F_{0.01}(1,15) = 8.68$);
*: Significant to 5% ($F_{0.05}(1,15) = 4.54$); NS : Not significant.

Similarly, the $P_s \times I_R$, $I_R \times F_T$, $P_s \times H_r$, $I_R \times H_r$, $F_T \times$ [AA] interactions and the quadratic interactions $F_T \times F_T$ and $H_r \times H_r$ also showed a significant effect on the response for a 95% confidence level.

For the second response (MB adsorbed), except the linear effect of particle size P_s, all other linear effects had a significant effect on the response at 95% confidence level. Similarly, for the quadratic effects $P_s \times P_s$, $I_R \times I_R$, and $F_T \times F_T$ reflect a significant effect at 99% confidence level. On the other hand, the $P_s \times I_R$, $P_s \times F_T$, $I_R \times F_T$, $F_T \times H_r$, $F_T \times$ [AA], $H_r \times$ [AA] interactions showed a significant effect on the response at 95% confidence level.

3.3. Modelization

For the study of the improvement and the optimization of the process (activated carbon preparation from grape seeds), it is necessary to use a polynomial model of second-degree at least [31].

The central composite design allowing the use of a second-degree polynomial model, which makes it possible to establish the equation of the following model:

$$Y = b_0 + b_1X_1 + b_2X_2 + b_3X_3 + b_4X_4 + b_5X_5 + b_{11}X_1^2 + b_{22}X_2^2 + b_{33}X_3^2 + b_{44}X_4^2 + b_{55}X_5^2 + b_{12}X_1X_2 + b_{13}X_1X_3 + b_{14}X_1X_4 + b_{15}X_1X_5 + b_{23}X_2X_3 + b_{24}X_2X_4 + b_{25}X_2X_5 + b_{34}X_3X_4 + b_{35}X_3X_5 + b_{34}X_4X_5 \quad (4)$$

where Y: the value of the calculated response, X_i: the value of the coded variable "i", b_i: The coefficient of the variable X_i model, b_{ii}: The coefficient of the model of the square variable X_i^2, b_{ij}: The coefficient of the interaction model between X_i and X_j.

This model has 10 terms:

- Constant term = 1,
- Linear term = 5,
- Square term = 5,
- Rectangle term = 10.

Taking into account the 95% confidence level and according to Tables 4 and 5, the non-significant coefficients for the responses are eliminated. Therefore, the model's equations are written as follows:

- Activated carbon yield (%):

$$\text{AC yield \%} = 29.725972 + 3.7791667P_s - 3.2675I_R - 4.836667F_T - 3.4525P_s \times I_R - 3.38I_R \times F_T + 3.34625\ P_s \times H_r - 3.98625I_R \times H_r + 2.405F_T \times [\text{AA}] - 3.210208F_T \times F_T - 4.252708H_r \times H_r \quad (5)$$

- Methylene blue adsorption capacity (mg/g):

$$\text{MB adsorption capacity} = 495.65701 - 5.567917I_R + 11.07875F_T + 3.2420833H_r + 2.8970833\ [\text{AA}] + 4.463125\ P_s \times I_R - 5.156875\ P_s \times F_T + 8.809375I_R \times F_T - 5.560625F_T \times H_r - 4.493125F_T \times [\text{AA}] + 2.841875H_r \times [\text{AA}] - 3.493021\ P_s \times P_s - 3.776771I_R \times I_R - 3.471771F_T \times F_T \quad (6)$$

3.4. Graphical study of the effect of the factors

The representative curves of the variation of activated carbon yield as a function of the factors studied show that the particle size has a positive effect on the yield (Fig. 2). On the other hand, the increase in the impregnation ratio and the final temperature decreases significantly the yield. These results confirm the research of Sudaryanto et al. [21] who showed that in the case of cassava peel the yield of AC decreases with the increase in the ratio of impregnation and it decreases from a carbonization temperature more than 650°C. González-García [23] reported that high temperature gives good char but decreases the yield. The increase in the concentration of the activating agent shows a slight variation in this response, while the increase in the concentration of the activating agent shows a slight variation in this response. Finally, a significant slope can be seen in the case of the heating rate, relative to optimal values of the response (AC yield = 30%).

The analysis of the factor's effects on the methylene blue adsorption capacity curves showed a significant effect of the impregnation ratio and the final temperature. Indeed, an increase in the final temperature increases the response (MB absorbed = 496.92 mg/g) while the increase in the impregnation ratio tends to decrease the MB adsorption capacity. On the other hand, the heating rate and the activating agent concentration have a slightly significant effect, while the effect of the particle size is not significant on the MB adsorption capacity. Similar results are reported by other researchers.

3.5. Validation of models

The quality of the adjustment of the model was verified by the coefficient of determination (R^2). In this case, the value of the coefficient of determination (R^2_{ACy} = 0.9247 and R^2_{MBa} = 0.9552) indicates that only 7.53% and 4.48% of the total variations for Activated carbon yield (%) and Methylene blue adsorption capacity are not explained by the regression models. In addition, very high values of the correlation coefficient (R_c = 0.9616 AC yield and R_c = 0.9773 MB adsorption) indicate a very good correlation between the estimated values and the experimental results. Similarly, Durbin-Watson statistics (DW_{ACy} = 2.24 and DW_{MBa} = 2.02) were found to be close to 2 indicating a good model fit.

The experimental values predicted values, and their differences are grouped in Table 6. After the analysis, it can be seen that there is no statistically significant difference between these values. In addition, Fig. 3 shows a good correlation between the predicted and experimental values for the 'AC yield and MB adsorption capacity responses, with very high values of the coefficient of determination R^2.

3.6. Optimization

Iso-response curves and response surfaces were generated by STATISTICA software to assess the relative effect of two factors when the other factors are held constant. Based on the regression equation, these representations are formed to understand the effects of the variables on the responses and also to determine the optimums for the

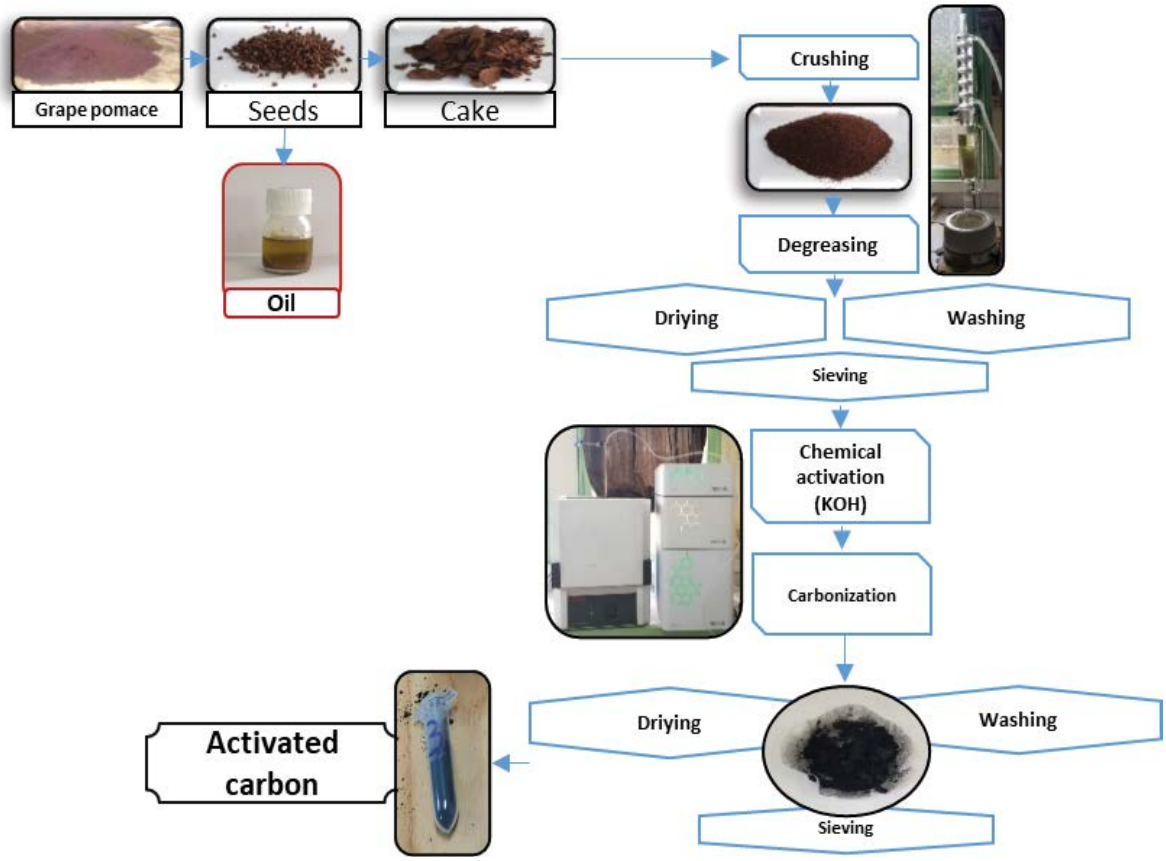

Fig. 2. Experimental procedures for the synthesis of activated carbon by chemical activation from grape seeds.

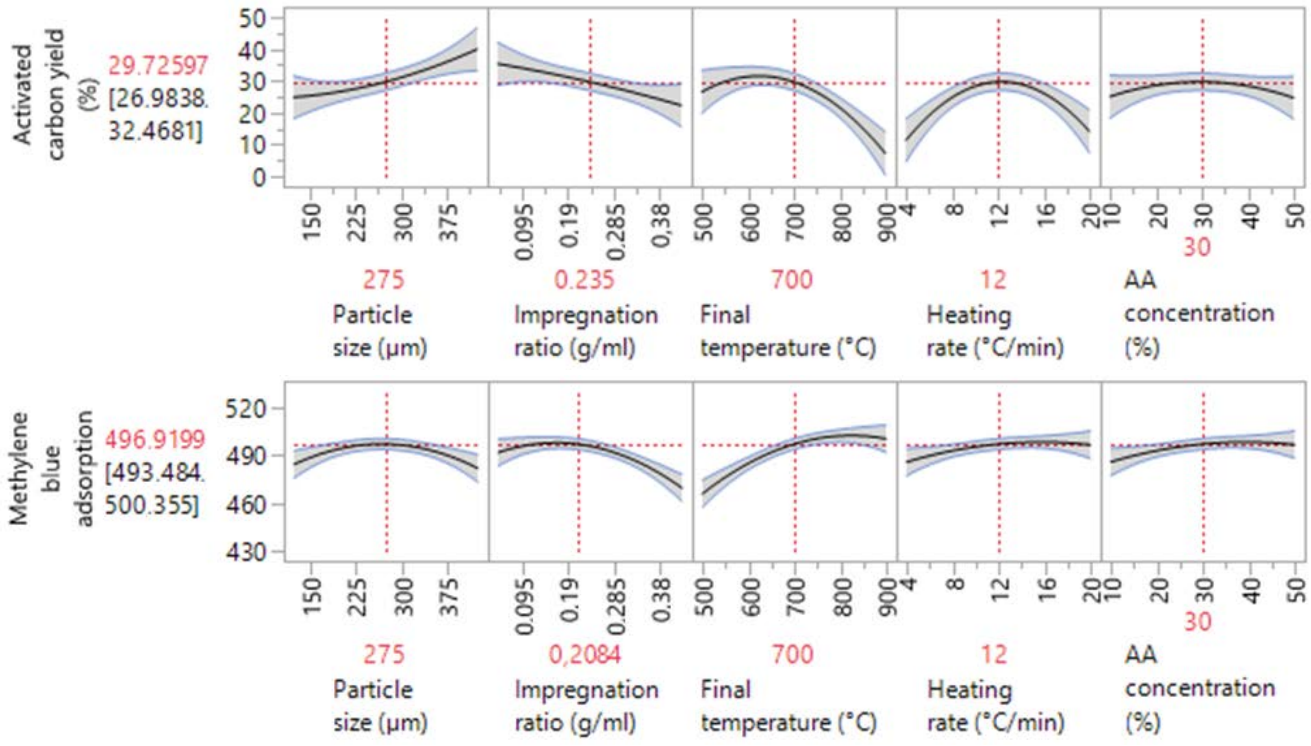

Fig. 3. Main effects plot of parameters on responses (activated carbon yield and Methylene blue adsorption capacity).

Table 6
Experimental results, calculated response and residual values for activated carbon yield and Methylene blue adsorption capacity responses

Actual order	AC yield %			MB adsorption (mg/g)		
	Calculated	Predicted	Residual	Calculated	Predicted	Residual
1	14.98	16.35	–1.37	470.61	473.89	–3.28
2	14.72	15.43	–0.71	497.47	499.76	–2.29
3	19.92	20.87	–0.95	497.79	497.45	0.34
4	20.22	17.57	2.65	495.97	494.54	1.43
5	26.31	31.16	–4.85	434.67	440.21	–5.54
6	21.75	22.99	–1.24	442.26	446.71	–4.45
7	11.65	13.13	–1.48	499.37	501.19	–1.82
8	3.6	4.42	–0.82	496.45	497.28	–0.83
9	25.91	26.50	–0.59	484.28	484.23	0.05
10	49.71	46.69	3.02	484.52	483.38	1.14
11	19.42	16.65	2.77	493.36	489.59	3.77
12	41.67	38.23	3.44	482.60	477.84	4.76
13	28.26	29.38	–1.12	448.10	450.21	–2.11
14	21.89	22.35	–0.46	487.99	489.11	–1.12
15	11.75	12.45	–0.70	494.94	493.43	1.51
16	13.04	10.14	2.90	496.05	493.45	2.60
17	29.34	24.89	4.45	487.89	480.41	7.48
18	35.44	40.01	–4.57	476.93	482.96	–6.03
19	31.32	35.39	–4.07	487.99	491.69	–3.70
20	26.26	22.32	3.94	474.56	469.41	5.15
21	30.28	26.56	3.72	467.68	459.61	8.07
22	3.37	7.21	–3.84	497.31	503.93	–6.62
23	15.51	11.30	4.21	486.13	483.33	2.80
24	9.8	14.13	–4.33	494.94	496.29	–1.35
25	22.09	25.09	–3.00	484.73	484.11	0.62
26	27.6	24.72	2.88	496.52	495.69	0.83
27	28.7	29.73	–1.03	498.10	495.66	2.44
28	29.75	29.73	0.02	493.14	495.66	–2.52
29	31.36	29.73	1.63	496.60	495.66	0.94
30	31.44	29.73	1.71	496.05	495.66	0.39
31	29.6	29.73	–0.13	493.36	495.66	–2.30
32	31.67	29.73	1.94	494.15	495.66	–1.51
33	26.96	29.73	–2.77	495.18	495.66	–0.48
34	28.02	29.73	–1.71	495.89	495.66	0.23
35	30.82	29.73	1.09	496.68	495.66	1.02
36	29.06	29.73	–0.67	495.97	495.66	0.31

responses studied. This means that the graphs are derived from the quadratic model equations.

The interaction effect of the variables for the efficiency of AC synthesis yield and methylene blue adsorption capacity is visualized through response surfaces and iso-response curves as shown in Figs. 4 and 5.

Thus, the response surfaces and iso-response curves for AC yield (Fig. 3) show the interaction effect of the final temperature and the impregnation ratio at fixed values of particle size (P_s = 300 μm), heating rate (R_H = 14°C/min) and activating agent concentration ([AA] = 35%). The results show a significant increase in the activated carbon yield (%) with the decrease in the impregnation ratio. On the other hand, the final temperature did not significantly affect the yield because the optimal values of the AC yield (%) were considered higher than 40%, for an impregnation ratio between 0.045 and 0.1 and a final temperature between 650°C and 800°C.

Response surfaces and iso-response curves of the relationships between the dependent response (Methylene blue adsorption capacity) and the independent variables, final temperature, and impregnation ratio when the particle size, heating rate, and activating agent concentration are kept constant are presented in Fig. 4. As shown in this

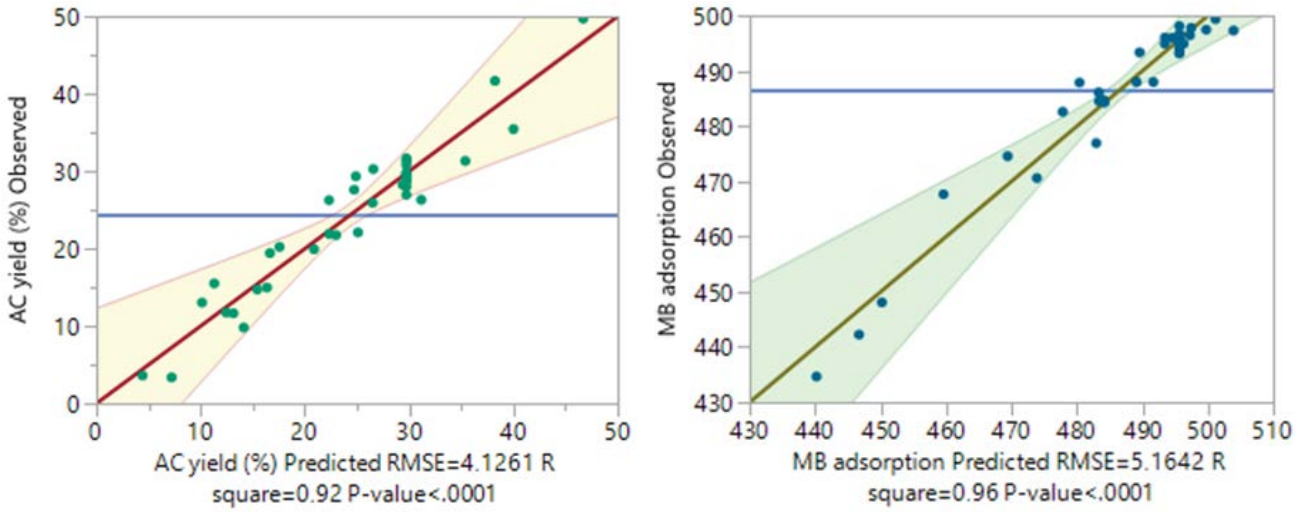

Fig. 4. Correlation between observed and predicted values of activated carbon yield and Methylene blue adsorption capacity.

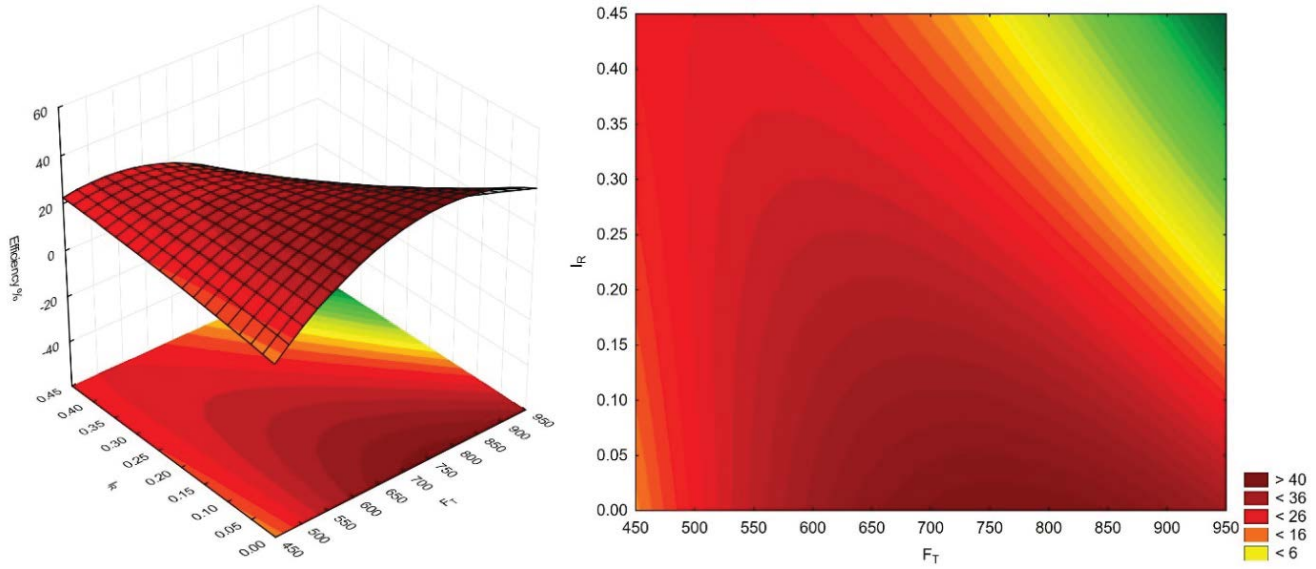

Fig. 5. Response surfaces and iso-response curves of activated carbon yield (%) as a function of final temperature and impregnation ratio.

figure, there is a strong interaction between the two factors I_R and F_T, since as they simultaneously increase the response increases, subsequently giving an optimal zone (MB adsorbed > 492 mg/g), relative to a final temperature between 600°C and 750°C and an impregnation ratio between 0.075 and 0.2. These results are explained by the fact that the higher concentrations of MB dye in the raw solution create a greater driving force to accelerate the movement of MB dye molecules to the active adsorption (binding) sites on the activated carbon surface [24]. On the other hand, the increase in MB removal with increasing AC dosage is due to the increased surface area of AC available in the solution. A higher adsorbent dosage also reflects a greater number of available active adsorption sites [25].

The main objective of the optimization is to determine the optimal values of the variables for the efficiency of the yield of activated carbon synthesis with optimal BM adsorption capacity, based on the model obtained from experimental data. For that, we superimposed the iso-response curve of the AC yield on the iso-response curve of MB adsorption capacity. The result obtained is shown in Fig. 6.

The analysis of this figure highlights the optimal areas that lead to the development of a grape seed-based activated carbon with optimal adsorbed MB capacity. From these optimal domains, we can notice that the predicted values of the synthesis yield of AC are between 35% and 40%, with a BM adsorbed between 495 and 500 mg/g. The conditions to reach these values are grouped in Table 7.

As shown by the results included in Table 9, adsorption using engineered activated carbon is an applicable technique for water treatment under reasonable operating conditions.

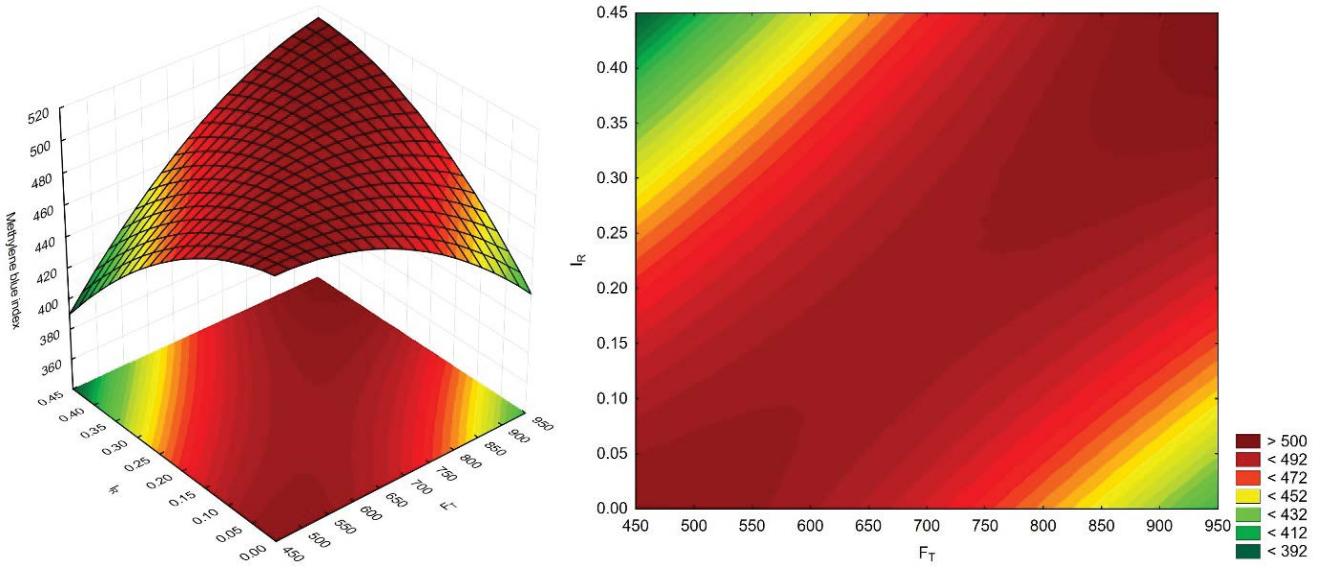

Fig. 6. Response surfaces and iso-response curves of Methylene blue adsorption as a function of final temperature and impregnation ratio.

Table 7
Optimal conditions for activated carbon preparation from grape seeds

Natural variables (X_j)	Symbol	Optimal value
X_1 = Particle size (µm)	P_s	300
X_2 = Impregnation ratio (g/mL)	I_R	0.045–0.15
X_3 = Final temperature (°C)	F_T	575–750
X_4 = Heating rate (°C/min)	H_r	14
X_5 = AA concentration (%)	[AA]	35

3.7. Experimental verification and characterization by FTIR spectroscopy and SEM

To verify that the experimental measurements of the responses are in agreement with what has been predicted, it is necessary to repeat the experiment at an optimal point, taking into account the optimal conditions relative to that point. The experiment is performed 3 times to ensure repeatability and to decrease the experimental error due to the experiment. Subsequently, these three experiments will be used to determine the significance of the difference between the experimental values and the predicted value.

The predicted value, the experimental values, and the difference between the values for the two responses at the optimal point is given in Table 8. The data shown in this table show that the differences between the predicted and experimental values are small. Therefore, the model established can be considered to be representative of the responses studied.

A Fourier transform infrared transmission spectrum (FTIR) was obtained to determine the characteristic bands of AC prepared from grape seeds (Fig. 7). Examination of this spectrum reveals the presence of several bands of absorption of valence and deformation vibrations attributable to the different groups existing in the synthesized material. Firstly, a wideband between 1,000 and 1,120 cm^{-1} is characteristic of the deformation in the plane of the aliphatic C–O [42]. A very small band at 1,392 cm^{-1} is related to the C–H deformations in the aliphatic chains [42,43]. A wideband at 1,637 to 1,645 cm^{-1} can most probably be related to the C=C elongations of olefins (alkenes) and aromatics [44]. One also observes the appearance of a very weak band at 1,730 cm^{-1} corresponding to the C=O function elongation vibration [43,44]. Similarly, Fig. 9 shows the surface morphology of activated carbon prepared under the optimal conditions. From this figure, the optimal conditions of activation temperature and

Table 8
Predicted values, experimental values, and residuals for the optimums of the two responses "Activated carbon yield and Methylene blue adsorption capacity"

AC yield (%)			MB adsorption (mg/l)		
$AC{\cdot}y_{experimental}$	$AC{\cdot}y_{predicted}$	$Y_{pr} - Y_{exp}$	$MB{\cdot}a_{experimental}$	$MB{\cdot}a_{predicted}$	$Y_{pr} - Y_{exp}$
38		–2	500		–3
36.5	40	–3.5	498.5	497	–1.5
41.6		1.6	497.3		–0.3

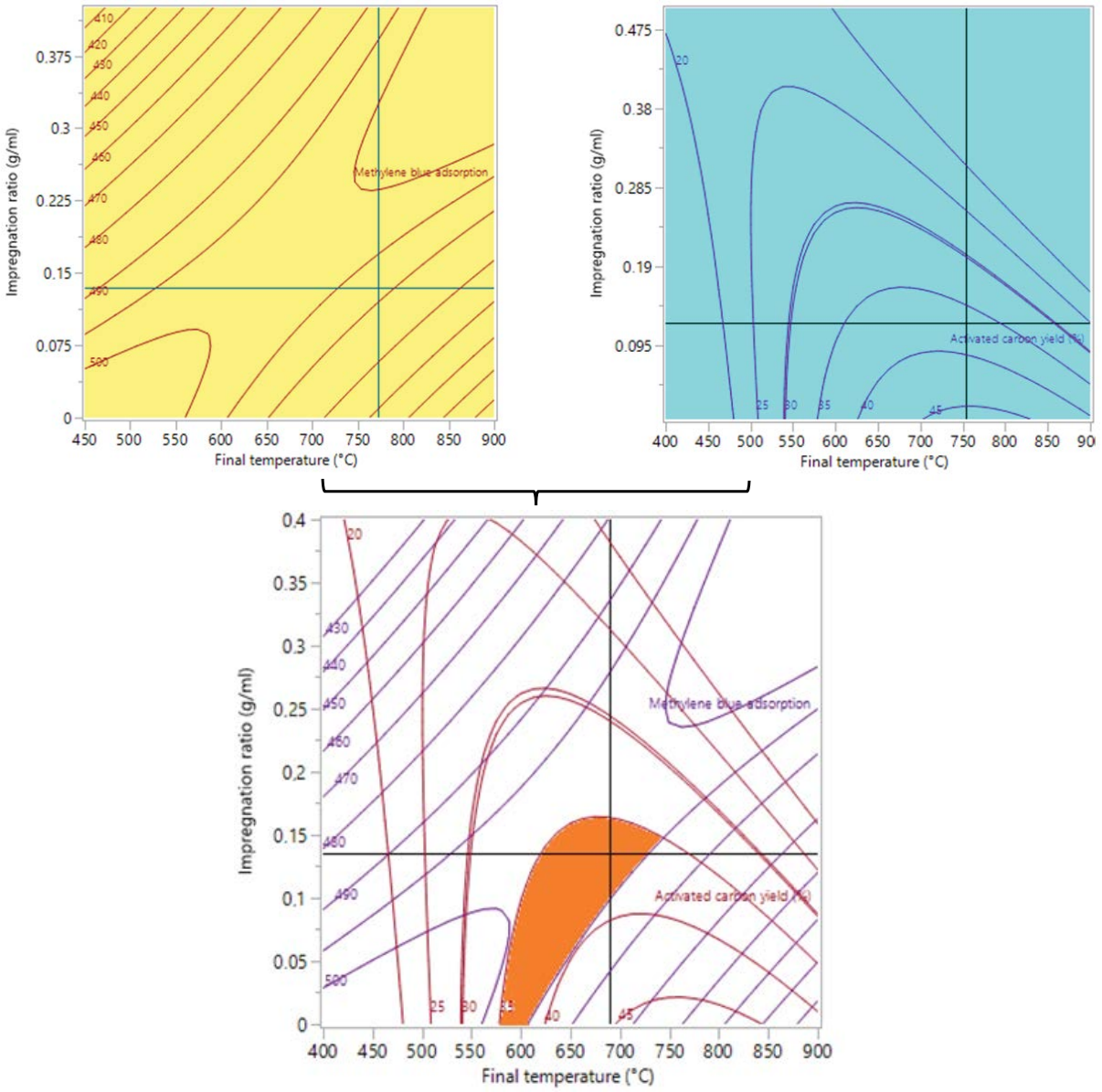

Fig. 7. Superposition of the iso-response curves of the two responses "Activated carbon yield and Methylene blue adsorption capacity".

Table 9
Comparison of adsorption capacities of MB on various adsorbents

Biomass waste	Activation agent	MB Adsorption capacity (mg/g)	Reference
Arundo donax	$ZnCl_2$	416.67	[34]
Albizia lebbeck seed pods	KOH	381.22	[35]
Jatropha curcas L. press-cake	KOH	393.06	[36]
Walnut shell	$ZnCl_2$	315.00	[37]
Coconut	H_3PO_4	250 mg/g	[38]
Banana peel	KOH	385.12	[39]
Pineapple waste biomass	$ZnCl_2$	288,34	[40]
Walnut	H_3PO_4	270.38	[41]
Grape seeds	KOH	492	This work

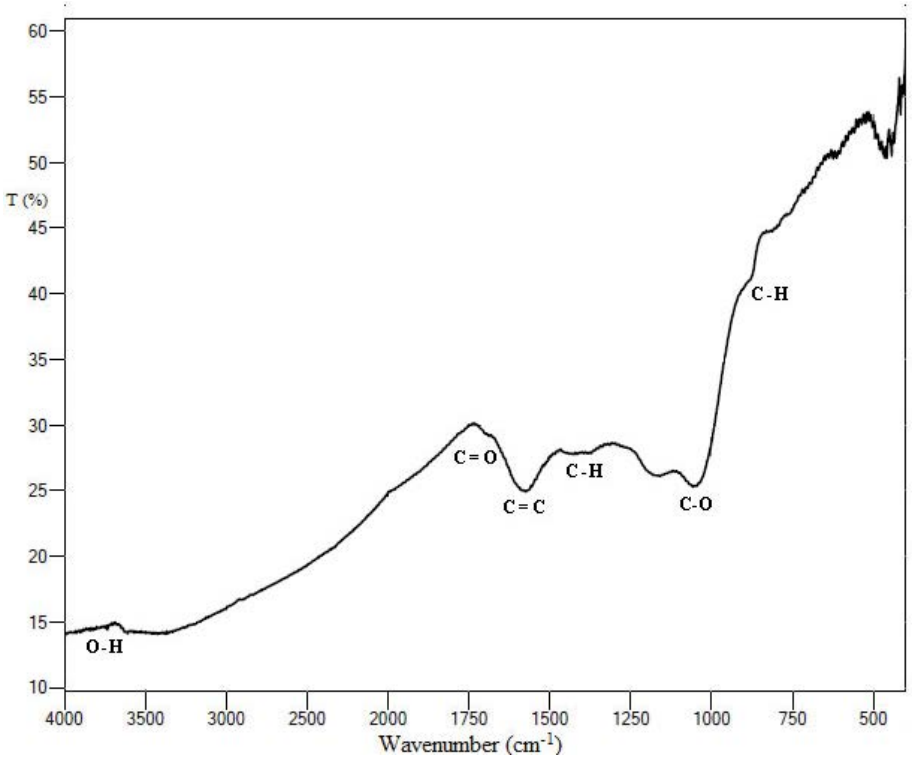

Fig. 8. Infrared absorption spectrum of activated carbon synthesized under optimal conditions.

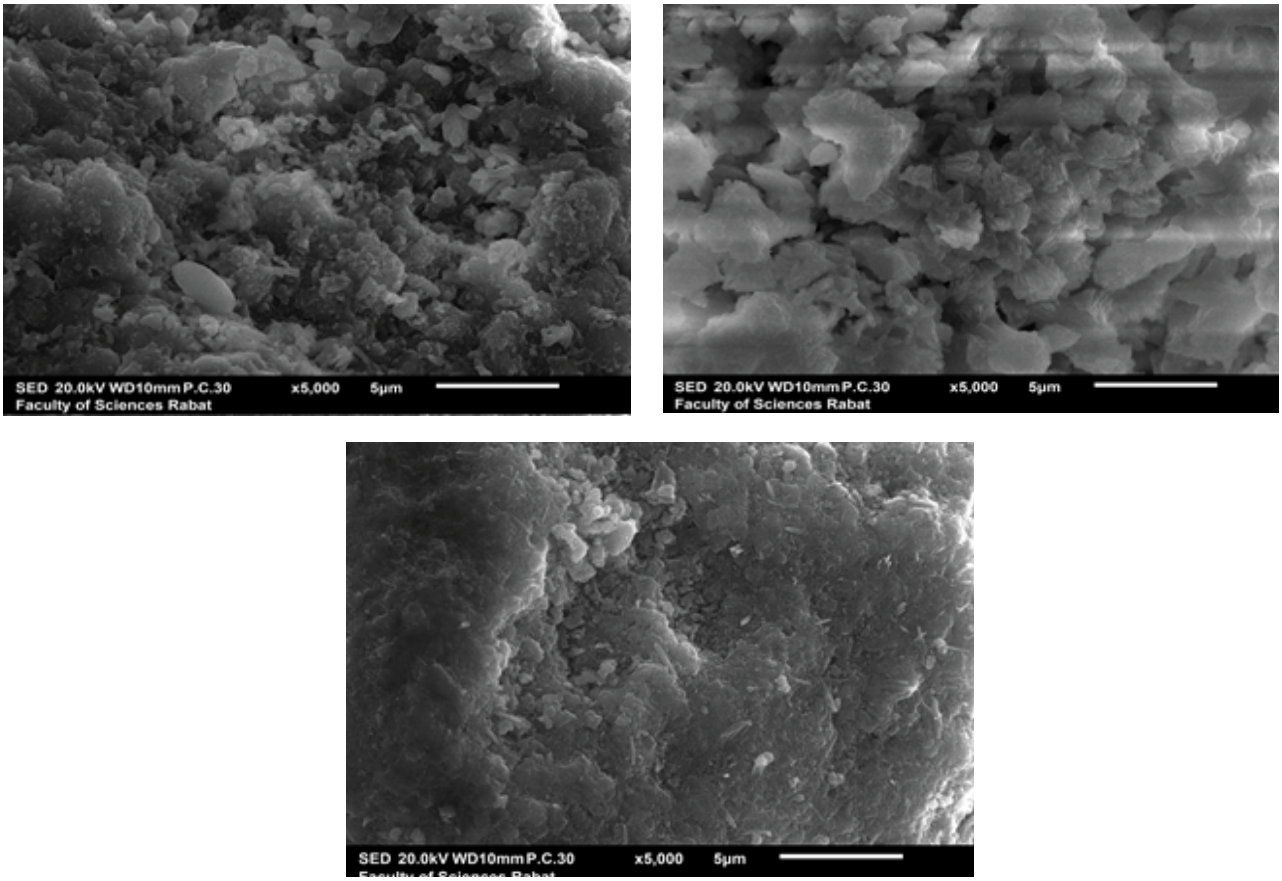

Fig. 9. SEM of activated carbon synthesized under optimal conditions.

impregnation rate were found to be more effective in creating well-developed pores on the surface of the resulting activated carbon, which seems to be the main factor that resulted in a higher adsorption capacity of methylene blue [25,45].

4. Conclusion

Experimental design methodology according to the response surface methodology was used to investigate the effects of five independent factors on the activated carbon yield (%) and adsorption capacity measured by methylene blue adsorption capacity in the preparation of activated carbons from grape seed using the chemical activation method. The influences of these various factors on the responses were modeled by a quadratic second-order model adequately, and response surface plots and iso-response curves are used to locate the optimal condition of activated carbon. Indeed, the optimal activated carbon from grape seed was obtained using a particle size of 300 μm, a final temperature of 650°C, an activating agent concentration of 35%, and an impregnation ratio of 0.15 g/mL, and a heating rate of 10°C/min, giving AC yield (%) higher than 40% and a methylene blue adsorption capacity higher than 492 mg/g.

Examination of the FTIR spectrum of the CA synthesized revealed the presence of several absorption bands of the valence and deformation vibrations attributable, a sign of the formation of activated carbon under the optimal conditions, also the SEM analysis shows the creation of pores on the surface of the resulting activated carbon. Consequently, this work successfully proposes a central composite design to optimize experimental conditions for the synthesis of activated carbon materials, which could be further employed in industrial applications.

References

[1] A.B. Siles-Castellano, M.J. López, J.A. López-González, F. Suárez-Estrella, M.M. Jurado, M.J. Estrella-González, J. Moreno, Comparative analysis of phytotoxicity and compost quality in industrial composting facilities processing different organic wastes, J. Cleaner Prod., 252 (2020) 119820, doi: 10.1016/j.jclepro.2019.119820.

[2] N. Unusan, Proanthocyanidins in grape seeds: an updated review of their health benefits and potential uses in the food industry, J. Funct. Foods, 67 (2020) 103861, doi: 10.1016/j.jff.2020.10386.

[3] C. Da Porto, E. Porretto, D. Decorti, Comparison of ultrasound-assisted extraction with conventional extraction methods of oil and polyphenols from grape (*Vitis vinifera* L.) seeds, Ultrason. Sonochem., 20 (2013) 1076–1080.

[4] Z.S. Khan, A. Mandal, S. Maske, T.P. Ahammed Shabeer, N. Gaikwad, S. Shaikh, K. Banerjee, Evaluation of fatty acid profile in seed and oil of Manjari Medika, a novel Indian grape cultivar and its comparison with Cabernet Sauvignon and Sauvignon Blanc, Sustainable Chem. Pharm., 16 (2020) 100253, doi: 10.1016/j.scp.2020.100253.

[5] J.C. Pierron, L'huile de pépins de raisin en France et dans le monde OCL, 24 (2017) 2017034, doi: 10.1051/ocl/2017034.

[6] A. Pal, K. Uddin, K. Thu, B.B. Saha, H.-S. Kil, S.-H. Yoon, J. Miyawaki, Synthesis of High Grade Activated Carbons from Waste Biomass, Encyclopedia of Renewable and Sustainable Materials, 2019, doi: 10.1016/B978-0-12-803581-8.11341-4.

[7] A.A. Mohd, A. Rasyidah, Optimization of rambutan peel based activated carbon preparation conditions for Remazol Brilliant Blue R removal, Chem. Eng. J., 168 (2011) 280–285.

[8] K.Y. Foo, B.H. Hameed, Microwave-assisted preparation of oil palm fibber activated carbon for methylene blue adsorption, Chem. Eng. J., 166 (2011) 792–795.

[9] B.S. Girgis, E. Smith, M.M. Louis, A.A. El-hendawy, Pilot production of activated carbon from cotton stalks using H_3PO_4, J. Anal. Appl. Pyrolysis, 86 (2009) 180–184.

[10] J. Guo, A.C. Lu, Characterization of adsorbent prepared from oil palm shell by CO_2 activation for removal of gaseous pollutants, Mater. Lett., 55 (2002) 334–339.

[11] M.A. Yahya, Z. Al-Qodah, C.W.Z. Ngah, Agricultural bio-waste materials as potential sustainable precursors used for activated carbon production: a review, Renewable Sustainable Energy Rev., 46 (2015) 218–235.

[12] K. Thu, Y.-D. Kim, A. Bin Ismil, B.B. Saha, K.C. Ng, Adsorption characteristics of methane on Maxsorb III by gravimetric method, Appl. Therm. Eng., 72 (2014) 200–205.

[13] M.N. Efimov, A.A. Vasilev, D.G. Muratov, A.E. Baranchikov, G.P. Karpacheva, IR radiation assisted preparation of KOH-activated polymer-derived carbon for methylene blue adsorption, J. Environ. Chem. Eng., 7 (2019) 103514, doi: 10.1016/j.jece.2019.103514.

[14] J.M.P. Torres, H.C. Sariol, J. Yperman, P. Adriaensens, R. Carleer, T.M. Peacok, Á.B. Sauvanell, E. Thijssen, G. Reggers, T. Haeldermans, P. Samyn, X-ray absorption as an alternative method to determine the exhausting degree of activated carbon layers in water treatment system for medical services, Talanta, 205 (2019) 120058, doi: 10.1016/j.talanta.2019.06.058.

[15] J. Rivera-Utrilla, M. Sánchez-Polo, Ozonation of 1,3,6-naphthalenetrisulphonic acid catalysed by activated carbon in aqueous phase, Appl. Catal., B, 39 (2002) 319–329.

[16] S. Wang, H. Nam, H. Nam, Preparation of activated carbon from peanut shell with KOH activation and its application for H_2S adsorption in confined space, J. Environ. Chem. Eng., 8 (2020) 103683, doi: 10.1016/j.jece.2020.103683.

[17] C.J. Gunes, A. Yakaboylu, T. Yumak, J.W. Zondlo, E.M. Sabolsky, J. Wang, Activated carbons prepared by indirect and direct CO_2 activation of lignocellulosic biomass for supercapacitor electrodes, Renewable Energy, 155 (2020) 38–52.

[18] F. Zietzschmann, G. Aschermann, M. Jekel, Comparing and modeling organic micro-pollutant adsorption onto powdered activated carbon in different drinking waters and WWTP effluents, Water Res., 102 (2016) 190–201.

[19] J. Rashid, F. Tehreem, A. Rehman, R. Kumar, Synthesis using natural functionalization of activated carbon from pumpkin peels for decolourization of aqueous methylene blue, Sci. Total Environ., 671 (2019) 369–376.

[20] K.T. Wong, N.C. Eu, S. Ibrahim, H. Kim, Y. Yoon, M. Jang, Recyclable magnetite-loaded palm shell-waste based activated carbon for the effective removal of methylene blue from aqueous solution, J. Cleaner Prod., 115 (2016) 337–342.

[21] Y. Sudaryanto, S.B. Hartono, W. Irawaty, H. Hindarso, S. Ismadji, High surface area activated carbon prepared from cassava peel by chemical activation, Bioresour. Technol., 97 (2006) 734–739.

[22] A.M.M. Vargas, C.A. Garcia, E.M. Reis, E. Lenzi, W.F. Costa, V.C. Almeida, NaOH-activated carbon from flamboyant (*Delonixregia*) pods: optimization of preparation conditions using central composite rotatable design, Chem. Eng. J., 162 (2010) 43–50.

[23] P.G. García, Activated carbon from lignocellulosics precursors: a review of the synthesis methods, characterization techniques and applications, Renewable Sustainable Energy Rev., 82 (2018) 1393–1410.

[24] A.S. Abdulhameed, N.N.M.F. Hum, S. Rangabhashiyam, A.H. Jawad, L.D. Wilson, Z.M. Yaseen, A.A. Al-Kahtani, Z.A. ALOthman, Statistical modeling and mechanistic pathway for methylene blue dye removal by high surface area and mesoporous grass-based activated carbon using K_2CO_3 activator, J. Environ. Chem. Eng., 9 (2021) 105530, doi: 10.1016/j.jece.2021.105530.

[25] A.H. Jawad, A.S. Abdulhameed, M.A.K.M. Hanafiah, Z.A. Alotman, M.R. Khan, S.N. Surip, Numerical desirability function for adsorption of methylene blue dye by sulfonated

pomegranate peel biochar: modeling, kinetic, isotherm, thermodynamic, and mechanism study, Korean J. Chem. Eng., 38 (2021) 1499–1509.
[26] A. Jaafar, A. Darchen, S. El Hamzi, Z. Lakbaibi, A. Driouich, A. Boussaoud, A. Yaacoubi, M. El Makhfouk, M. Hachkar, Optimization of cadmium ions biosorption by fish scale from aqueous solutions using factorial design analysis and Monte Carlo simulation studies, J. Environ. Chem. Eng., 8 (2020) 104727, doi: 10.1016/j.jece.2020.104727.
[27] J. Rashid, F. Tehreem, A. Rehman, R. Kumar, Synthesis using natural functionalization of activated carbon from pumpkin peels for decolourization of aqueous methylene blue, Sci. Total Environ., 671 (2019) 369–376.
[28] J. Goupy, L. Creighton, Introduction aux plans d'expériences, 3e edition, Dunod, Paris, 2006, ISBN 2 100 497 8.
[29] JMP version 11: Using JMP, SAS Institute, Cary, NC, 2013.
[30] C. Weiß, StatSoft, Inc., Tulsa, OK: STATISTICA, Version 8, AStA Advances in Statistical Analysis, 91 (2007) 339–341.
[31] A. Driouich, S. El Alami El Hassani, H. Labjar, S. Kassbi, T.K. Ntambwe, O. Britel, B. Sallek, K. Digua, R. Chroqui, H. Chaair, Modeling and optimizing synthesis of irreversible gel by sol-gel using experimental design, Phosphorus, Sulfur Silicon Relat. Elem., 195 (2020) 50–59.
[32] L. Eriksson, Design of Experiments: Principles and Applications, MKS Umetrics AB, Sweden, 2008.
[33] A. Driouich, F. Chajri, S.E.A. El Hassani, O. Britel, S. Belouafa, A. Khabbazi, H. Chaair, Optimization synthesis geopolymer based mixture metakaolin and fly ash activated by alkaline solution, J. Non-Cryst. Solids, 544 (2020) 120197.
[34] O. Üner, Hydrogen storage capacity and methylene blue adsorption performance of activated carbon produced from *Arundo donax*, Mater. Chem. Phys., 237 (2019) 121858, doi: 10.1016/j.matchemphys.2019.121858.
[35] M.J. Ahmed, S.K. Theydan. Optimization of microwave preparation conditions for activated carbon from Albizia lebbeck seed pods for methylene blue dye adsorption, J. Anal. Appl. Pyrolysis, 105 (2014) 199–208.
[36] A. Kurniawan, S. Ismadji. Potential utilization of *Jatropha curcas* L. press-cake residue as new precursor for activated carbon preparation: application in methylene blue removal from aqueous solution, J. Taiwan Inst. Chem. Eng., 42 (2011) 826–836.
[37] Y. Qiongfen, L. Ming, J. Xu, Q. Yu, Z. Yuntao, L. Congbin, Characterization and methanol adsorption of walnut shell activated carbon prepared by KOH activation, J. Wuhan Univ. Technol. Mater. Sci. Ed., 31 (2016) 260–268.
[38] A.H. Jawad, S. Sabar, M.A.M. Ishak, L.D. Wilson, S.S.A. Norrahma, M.K. Talari, A.M. Farhan, Microwave-assisted preparation of mesoporous-activated carbon from coconut (*Cocos nucifera*) leaf by H_3PO_4-activation for methylene blue adsorption, Chem. Eng. Commun., 204 (2017) 1143–1156.
[39] R. Liu, Y. Liu, X.Y. Zhou, Z.Q. Zhang, J. Zhang, F.Q. Dang, Biomass-derived highly porous functional carbon fabricated by using a free-standing template for efficient removal of methylene blue, Bioresour. Technol., 154 (2014) 138–147.
[40] M.N. Mahamad, M.A.A. Zaini, Z.A. Zakaria, Preparation and characterization of activated carbon from pineapple waste biomass for dye removal, Int. Biodeterior. Biodegrad., 102 (2015) 274–280.
[41] Y. Elmaguanaa, N. Elhadiri, M. Bouchdoug, M. Benchanaa, A. Jaouad, Optimization of preparation conditions of activated carbon from walnut cake using response surface methodology, Elmaguana & al./Mor. J. Chem., 6 (2018) 92–105.
[42] E. Koseoglu, C. Akmil-Basar, Preparation, structural evaluation and adsorptive properties of activated carbon from agricultural waste biomass, Adv. Powder Technol., 26 (2015) 811–818.
[43] O.V. Ovchinnikov, A.V. Evtukhova, T.S. Kondratenko, M.S. Smirnov, V.Y. Khokhlov, O.V. Erina, Manifestation of intermolecular interactions in FTIR spectra of methylene blue molecules, Vib. Spectrosc., 86 (2016) 181–189.
[44] S. Karimi, J. Feizy, F. Mehrjo, M. Farrokhnia, Detection and quantification of food colorant adulteration in saffron sample using chemometric analysis of FT-IR spectra, RSC Adv., 6 (2016) 23085–23093.
[45] M. Bardhan, T.M. Novera, M. Tabassum; M.A. Islam; A.H. Jawad, M.A. Islam, Adsorption of methylene blue onto betel nut husk-based activated carbon prepared by sodium hydroxide activation process, Water Sci. Technol., 82 (2020) 1932–1949.